Harmonic Auto-Regularization for Non Rigid Groupwise Registration in Cardiac Magnetic Resonance Imaging

S. Sanz-Estébanez[1], J. Royuela-del-Val[1], T. Sevilla[2], A. Revilla-Orodea[2],
S. Aja-Fernández[1], C. Alberola-López[1]

[1] Laboratorio de Procesado de Imagen (LPI), Universidad de Valladolid
[2] Instituto de Ciencias del Corazón (ICICOR). Hospital Clínico Universitario de Valladolid.

Abstract

In this paper we present a new approach for non rigid groupwise registration of cardiac magnetic resonance images by means of free-form deformations, imposing a prior harmonic deformation assumption. The procedure proposes a primal-dual framework for solving an equality constrained minimization problem, which allows an automatic estimate of the trade-off between image fidelity and the Laplacian smoothness terms for each iteration. The method has been applied to both a 4D extended cardio-torso phantom and to a set of voluntary patients. The accuracy of the method has been measured for the synthetic experiment as the difference in modulus between the estimated displacement field and the ground truth; as for the real data, we have calculated the Dice coefficient between the contour manual delineations provided by two cardiologists at end systolic phase and those provided by them at end diastolic phase and, consequently propagated by the registration algorithm to the systolic instant. The automatic procedure turns out to be competitive in motion compensation with other methods even though their parameters have been previously set for optimal performance in different scenarios.

1 Introduction

Image registration, to put it short, is concerned with the search of an optimal transformation for the alignment of at least two images. It has many applications in imaging, such as fusion of image information [1], material points tracking [2], atlas construction [3], or object-based interpolation of contiguous slices [4]. As for the groupwise registration problem, it may be posed as finding a mutual transformation τ so that every point in each image is matched to a point in a reference image that is built out of the whole image set to be registered; the transformation is found as the minimization in the space of possible transformations of an energy function H, i.e., the registration looks for the optimal transformation that satisfies $\tau^* = \arg\min_{\tau} H(\tau)$.

The energy function associated to the transformation comprises two competing goals. The first term represents the cost associated with the image similarity (i.e., the data fidelity term). Examples of common voxel-based similarity measures are cross correlation [5], mutual information [6] or mean squared differences, which have proved their usefulness either in monomodal or multimodal image alignment problems. On the other hand, the second term corresponds to the cost associated to the smoothness of the transformation. Most common smoothness terms try to favour those solutions in which the first or second-order derivatives of the displacement field tend to zero (membrane or plate-like solutions) [7, 8] or can be based on a biomechanical model of deformation [9].

An incorrect use of the smoothness term could result in unrealistic transformations; therefore, a proper set of additional constraints that assures certain properties such as continuity or differentiability should be introduced in the problem for a correct definition. Therefore, a parameter λ is often introduced as a trade-off between data fidelity and transformation smoothness. Clearly, this parameter will play a major role in the final result, so it should be set beforehand on the basis of some optimality conditions, requiring some fine tuning to estimate the optimal value. This is a time consuming process that may have to be repeated according to acquisition protocol, type of pathology, etc.

In this paper, we have developed an extension of the framework presented in [10] for its application to non-rigid registration of cardiac magnetic resonance imaging (MRI), that combines the advantages of voxel-based monomodal measures, such as mean squared differences, with a non rigid transformation model described by free-form deformations (FFD) based on B-splines [11], in which the trade-off between the data fidelity term, related to the monomodal metric, and the regularization term, related to the smoothness of transformation, is automatically set due to an harmonic constraint term.

2 Materials and Methods

2.1 Materials

For the validation of the proposed approach, a synthetic experiment has been carried out using a simulation environment based on the 4D digital extended cardio-torso (XCAT) phantom [12]. The phantom consists of a whole body model that contains high level detailed anatomical labels, which feed a high resolution image synthesis procedure, providing different modalities such as CT, MRI and PET. The 4D XCAT phantom incorporates state of the art respiratory and cardiac mechanics, which provide

ISBN: 978-84-9048-531-6

sufficient flexibility to simulate cardio-torso motion from user-defined parameters. Therefore, the phantom provides us not only with the images themselves, but also with a ground-truth displacement field.

Additionally, we have performed cardiac studies in a population of 74 subjects, 46 of which are affected by primary or secondary forms of hypertrophic cardiomyopathy (HCM) [13] and a control group that consists of 28 healthy volunteers. A short axis (SA) SENsitivity ENcoding (SENSE) balanced Turbo Field Echo MR-Cine sequence has been acquired on a Philips Achieva 3T scanner for each patient, where the myocardium contours have been manually traced by two cardiologists at end-diastole (ED) and end-systole (ES) phases. The latter will be taken as ground truth for the experiments described in section 3 on real images. Acquisition and resolution details for these experiments are shown in Table 1.

Parameters	XCAT	MR-Cine
Δ_p	1	0.96-1.18
Δ_l	8	8
N_p	256	240-320
N_t	20	30
N_s	16	10-15
T_R	3	2.9-3.918
T_E	1.5	1.45-2.22
α	60	45
Card.	1	~ 1
Resp.	5	Navig.

Table 1. *Details on the image sequences used in this paper. Δ_p : Spatial Resolution (mm). Δ_l : Slice Thickness (mm). N_p : Number of pixels along each direction. N_t: Number of Temporal Phases. N_s: Number of slices. T_R : Repetition Time (ms). T_E : Echo Time (ms). α: Flip Angle (°). $Card.$: Cardiac Period (s). $Resp.$: Respiratory Period (s).*

2.2 Methods

The proposed method has been applied to the groupwise registration of two-dimensional cardiac MR-Cine acquisitions and, specifically, for contour propagation across different cardiac phases. Many potential uses of this procedure can be considered, such as motion compensated compressed sensing accelerated reconstruction [14].

Bearing in mind the aforementioned application, the local transformation τ is represented as a combination of B-spline FFDs. Bilinear interpolation is used to obtain the intensity of the deformed MR-Cine images on a rectilinear grid [15]. A gradient-descent optimization scheme is performed, where the step size is updated according to the variation in the registration metric. The sum of the squared differences of the image intensity, over a region of interest (ROI) denoted as χ, is used as the registration metric as follows:

$$H(\tau) = \int_{\chi} \frac{1}{N} \sum_{n=1}^{N} \left(I_n(\mathbf{x}, \tau_n) - \frac{1}{N} \sum_{n=1}^{N} I_{n'}(\mathbf{x}, \tau_{n'}) \right) d\mathbf{x} \quad (1)$$

In general, the local deformation of cardiac tissue should be characterized by a smooth transformation. To constrain the spline-based FFD transformation to be smooth, a penalty term which regularizes the transformation is introduced. We have resorted to harmonic regulation, i.e., $\nabla^2(\tau) = 0$; in computer vision, the Laplacian operator has been used for various tasks such as blob and edge detection [16] and its quantity determines the density of the gradient flow of the displacement field, which is associated with the smoothness of the transformation.

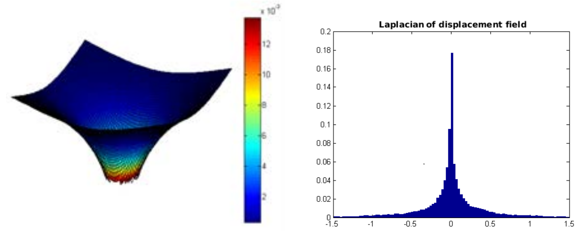

(a) (b)

Figure 1. *The figure on the left shows an example of Laplacian field coloured by its first order smoothness. The figure on the right shows the histogram of the components of the Laplacian of the transformation in a medial slice of a healthy volunteer.*

An harmonic constraint seems acceptable for cardiac motion compensation, as non-regularized solutions, as shown in Figure 1(b), present a noticeable tendency towards harmonic fields. Therefore, it should provide an appropriate level of smoothness over the transformation so as to avoid registration artifacts. With such constraints, the minimization problem would be formulated as:

$$\text{minimize} \quad H(\tau) \quad \text{subject to} \quad \nabla^2(\tau) = 0. \quad (2)$$

Introducing the primal-dual framework [10], we can consider the quadratic penalty problem associated with (2) as:

$$\text{minimize} \quad H(\tau) + \frac{\lambda}{2} ||\nabla^2(\tau)||^2. \quad (3)$$

Imposing the first order necessary optimality condition (null gradient), this problem can be posed as:

$$\nabla H(\tau) + \lambda A(\tau)^T \nabla^2(\tau) = 0, \quad (4)$$

where $A(\tau)$ is the Jacobian matrix of vector $\nabla^2(\tau)$.

These conditions can be rewritten under the form:

$$F(\tau, y, \mu) = \begin{pmatrix} \nabla H(\tau) + A(\tau)^T y \\ \nabla^2(\tau) - \mu y \end{pmatrix} = 0, \quad (5)$$

where y is a vector of Lagrangian multipliers and μ is inversely related with λ, used for notation convenience.

The equation (5) implicitly defines a trajectory for μ such that $\tau(\mu \to 0) = \tau^*$ and $F(\tau(\mu), y(\mu), \mu) = 0$ for sufficiently small values of μ. Now, we can apply a Newton-like method to equation (5) to obtain a sequence that makes μ tend to 0. The linearization of (5) at the current iterate (τ_k, y_k, μ_k) provides an updating for these variables (also λ) that can be extracted from the following linear system:

$$J(\Delta\tau, \Delta y, \mu_k) + \frac{\partial F(\tau_k, y_k, \mu_k)}{\partial \mu} \Delta\mu = -F(\tau_k, y_k, \mu_k), \quad (6)$$

ISBN: 978-84-9048-531-6

where Δ represents the iterative increment of the variable, such as $\Delta y = y_{k+1} - y_k$ and J is the Jacobian matrix of the function F at k-iteration, or an approximation to it.

With such a design, the value of λ would increase as $\mu \rightarrow 0$ until registration converges; therefore, first iterations will let the transformation evolve unsmoothly until the harmonic regularization term becomes dominant owing to λ.

3 Results

In this Section, we test the accuracy of our automated regularization method in comparison with other methods that use a previously-set non-variable λ parameter. The latter methods are two, namely, one that considers first-order regularization both in the spatial and the temporal dimension, as in [7], and a second one which uses harmonic regularization, as we do, but with a unique λ that is set before the optimization takes place.

We have carried out a synthetic experiment with the data provided by the XCAT phantom on which we have measured the error of the estimation of cardiac displacement field (on a previously defined ROI). The optimal λ parameters for the whole myocardium have been empirically set to $\lambda = 0.007$ for the harmonic regularization and $\lambda_s = 0.3$ (spatial) and $\lambda_t = 0.1$ (temporal) for the first-order regularization; those parameters have provided the best results by visual inspection.

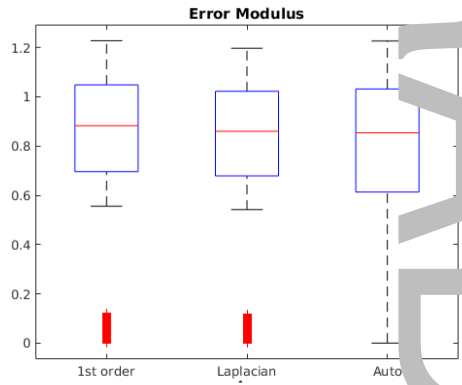

Figure 2. *Boxplot diagrams of error modulus in mm for estimated displacement field at myocardial points.*

In Figure 2 we show the boxplot diagrams of the distributions of the differences in modulus between the estimated 2-D displacement field and the ground-truth as a measure of accuracy. Accuracy for all these methods seems suitable for motion estimation as in most myocardial points error is lower than pixel resolution. Nevertheless, the automated procedure gives comparable results with the other two; specifically, no significant differences were found between these methods either in displacement error measures or in overlapping indices (Dice coefficient [17]) measured from the propagated segmentations.

In addition, for the real data we have tested the ability of the aforementioned procedures to propagate the manual segmentations (at ED phase) throughout the cardiac cycle. In this experiment, we have performed a quantitative analysis of the overlapping using the Dice coefficient between the propagated segmentations and the ground-truth at ES phase for each patient. As for the choice of λ, we have made a distinction between HCM and healthy cases, since this pathology greatly affects the characteristics of cardiac motion [13]; for each group this parameter has been set by visual inspection on a representative patient and then we have used this value for the remaining patients of the group. This is due to the fact that for all them the acquisition protocol has remained unchanged; in addition, the registration procedure has been run on a medial slice, where variability is much lower than in apical or basal slices.

In Figure 3 we show the boxplot diagrams of the Dice coefficient obtained from the aforementioned non variable methods with optimal settings and our automated regularization proposal. The optimal λ parameters for the harmonic regularization method were $\lambda = 0.2$ for HCM patients and $\lambda = 0.5$ for the control group, while for the first order regularization method; $\lambda_s = 1, \lambda_t = 3$ for HCM patients and $\lambda_s = 3, \lambda_t = 8$ for the control group [15].

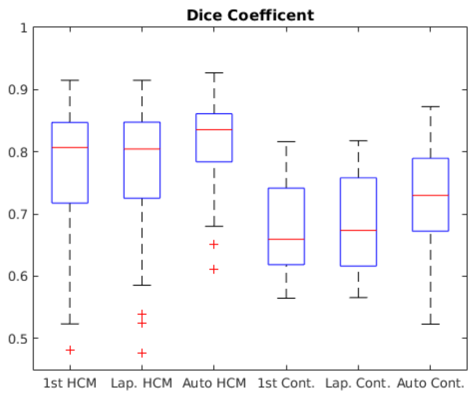

Figure 3. *Boxplot diagrams of Dice Coefficient distributions of propagated segmentations to ES and ground-truth segmentations.*

As observed in Figure 3, the automated procedure shows a considerable improvement in terms of overlapping compared with the other two methods, both for HCM patients and healthy volunteers, even though λ has been selected *ad-hoc* for each group. Mann-Whitney U-tests have been performed on the Dice coefficient distributions, finding significant improvements when using the auto-regularization method both over first order regularization ($p = 0,0254$ for HCM and $p = 0,042$ for controls) and harmonic regularization methods ($p = 0,0351$ for HCM and $p = 0,0512$ for control groups). These results highlight that a proper criterion of accommodation of the regularization parameter may enhance the development of registration algorithms in comparison with fixed, albeit optimal, parameters.

Furthermore, better performance figures are obtained for HCM patients in comparison with those from controls; in our opinion, this may be due to the fact that this particular pathology implies a loss of the myocardial functionalities leading into myocardial thickening, specially in the septum, as well as to a significant reduction of cardiac deformation [13]; this combined effects seem to ease motion compensation and segmentation propagation and, conse-

ISBN: 978-84-9048-531-6

quently, improving overlap indexes.

4 Conclusions and Future Work

We have presented an image processing methodology for non-rigid registration of cardiac MRI based on a primal-dual framework with harmonic constrained minimization that iteratively calculates the trade-off between the two terms involved in the problem. This methodology combined with the use of simple registration metrics under the groupwise paradigm has proven to be reliable in the propagation of manual segmentations through the cardiac cycle and accurate in the estimation of cardiac displacement fields, being useful as a motion compensation technique.

The automated procedure for the update of weighting parameters has been successfully tested in different scenarios with different grades of regularization requirements, significantly improving the performance obtained with optimized fixed weighting parameters procedures.

Finally, more complicated multimodal metrics, such as the one proposed in [18], could help to perform topology preserving registration in highly artifacted images, such as the typically observed in echo planar abdominal diffusion acquisitions.

5 Acknowledgments

This work was partially supported by the Spanish Ministerio de Ciencia e Innovación under Research Grant TEC2013-44194-P, the European Regional Development Fund (ERDF-FEDER) under Research Grant TEC2014-57428-R and the Spanish Junta de Castilla y León under Grant VA069U16.

References

[1] L. Cordero-Grande, S. Merino-Caviedes, X. Albà, RM. Figueras i Ventura, AF. Frangi, and C. Alberola-López. 3D Fusion of Cine and Late-Enhanced Cardiac Magnetic Resonance Images. In *9th IEEE ISBI*, pages 286–289, Barcelona, Spain, 2012.

[2] MJ. Ledesma-Carbayo, A. Bajo, C. Santa-Marta, E. Perez-David, I. Caso, MA. Garcia-Fernandez, A. Santos, and M. Desco. Cardiac Motion Analysis from Cine MR Sequences Using Non-Rigid Registration Tecniques. In *Computers in Cardiology*, pages 520–523, Valencia, Spain, 2006.

[3] GG. Fonseca, M. Backhaus, DA. Bluemke, RD. Britten, JD. Chun, BR. Cowan, ID. Dinov, JP. Finn, PJ. Hunter, AH. Kadish, DC. Lee, JAC. Lima, P. Medrano-Gracia, K. Shivkumar, A. Suinesiaputra, and AA. Young. The Cardiac Atlas Project: An imaging database for computational modeling and statistical atlases of the heart. *Bioinformatics*, 27, 2011.

[4] L. Cordero-Grande, G. Vegas-Sánchez-Ferrero, P. Casaseca-de-la-Higuera, and C. Alberola-López. A Markov Random Field Approach for Topology-Preserving Registration: Application to Object-Based Tomographic Image Interpolation. *IEEE Trans. On Image Proc.*, 21:2047 – 2061, 2012.

[5] BB. Avants, CL. Epstein, M. Grossman, and JC. Geel. Symmetric Diffeomorphic Image Registration with Cross-Correlation: Evaluating Automated Labeling of Elderly and Neurodegenerative Brain. *Med. Image Anal.*, 12:26–41, 2008.

[6] D. Mattes, DR. Haynor, H. Vesselle, T. Lewellen, and W. Eubank. Non-rigid multimodality image registration. *Med. Imag. 2001: Image Proc.*, 4322:1609–1620, 2001.

[7] D. Rueckert, LI. Sonoda, C. Hayes, DLG. Hill, MO. Leach, and DJ. Hawkes. Nonrigid Registration using Free-Form Deformations: Application to breast MR images. *IEEE Trans. Med. Imag.*, 18:712–721, 1999.

[8] MJ. Ledesma-Carbayo, JA. Derbyshire, S. Sampath, A. Santos, M. Desco, and ER. McVeigh. Unsupervised Estimation of Myocardial Displacement From Tagged MR Sequences Using Nonrigid Registration. *Magnetic Resonance in Medicine*, 59:181–189, 2006.

[9] N. Tustison and B. Avants. Explicit B-spline regularization in diffeomorphic image registration. *Frontiers in Neuroinformatics*, 7:39, 2013.

[10] P. Armand, J. Benoist, R. Omheni, and V. Pateloup. Study of a primal-dual algorithm for equality constrained minimization. *Computational Optimization and Applications*, 59:405–433, 2014.

[11] D. Rueckert, P. Aljabar, RA. Heckemann, JV. Hajnal, and A. Hammers. Diffeomorphic registration using b-splines. *MICCAI 2006*, 4191:702–709, 2006.

[12] WP. Segars, G. Sturgeon, S. Mendonca, J. Grimes, and BMW. Tsui. 4D XCAT phantom for multimodality imaging research. *Medical Physics*, 37:4902–4915, 2010.

[13] BJ. Baron. The 2006 American Heart Association Classification of Cardiomyopathies Is the Gold Standard. *Circ. Heart Fail.*, 1:72–76, 2008.

[14] J. Royuela-del-Val, L. Cordero-Grande, F. Simmross-Wattenberg, M. Martín-Fernández, and C. Alberola-López. Jacobian Weighted Temporal Total Variation for Motion Compensated Compressed Sensing Reconstruction of Dynamic MRI. *Magnetic Resonance in Medicine*, 2016.

[15] S. Sanz-Estébanez. Esquema de compensación de movimiento mediante registrado grupal aplicado a imagen cardiaca dinámica. Master's thesis, Universidad de Valladolid, Spain, 2014.

[16] D. Marr and E. Hildreth. Theory of Edge Detection. *Proceedings of the Royal Society of London. Series B, Biological Sciences*, 207:187–217, 1980.

[17] LR. Dice. Measures of the Amount of Ecologic Association Between Species. *Ecology*, 26:297–302, 1945.

[18] L. Cordero-Grande, S. Merino-Caviedes, S. Aja-Fernández, and C. Alberola-López. Groupwise elastic registration by a new sparsity-promoting metric: application to the alignment of cardiac magnetic resonance perfusion images. *IEEE Trans. Pattern Anal. Mach. Intell.*, 35:2638–2650, 2013.